UDC 539.4

Influence of H_2S Corrosion on Tensile Properties and Fracture Toughness of X80 Pipeline Steel

L. Gu, J. Wang,[1] C. B. Luan, and X. Y. Li

Department of Mechanical Engineering and Applied Electronics Technology, Beijing University of Technology, Beijing, China

[1] wjing@bjut.edu.cn

Tensile and fracture properties of X80 pipeline steel were studied in a mimic petrochemical environment. X80 pipeline steel specimens were firstly exposed to air or H_2S corrosive medium. Then their tensile properties and $\delta - \Delta a$ resistance curves were obtained in experiments. The influence of H_2S corrosion on the X80 pipeline steel's crack growth resistance curve, fracture toughness, and plastic work loss was analyzed. The comparison between the test results after two pretreatments indicates that there was no significant difference in the X80 pipeline steel's ultimate tensile strength before and after H_2S corrosion. But fracture elongation, area reduction and fracture toughness varied greatly (a substantial decrease in elongation and reduction of area). The crack growth resistance curve of the specimen in air was obviously higher than the crack growth resistance curve of the corroded one. Under stable crack growth stage, the crack initiation toughness $\delta_{0.2BL}$ of the specimen in air was 0.732 mm, 2.02 times that of the corroded one (0.364 mm). In the case of similar crack growth Δa, the plastic work required in the crack growing process (U_P) of the specimen in air was 2.29 times that of the H_2S-corroded specimen (U'_P). H_2S corrosion resulted in a significant reduction of the fracture toughness of X80 pipeline steel. Hence, H_2S corrosion should be avoided in the process of natural gas transportation by pipelines, so as to protect the pipeline steel from toughness degradation.

Keywords: X80 pipeline steel, tensile properties, resistance curve, fracture toughness, H_2S corrosion.

Introduction. The X80 pipeline steel is widely adopted in oil-and-gas pipelines of the Second West-East Pipeline Project in China, with a total length exceeding 7,000 km [1]. However, a safe operation of gas pipelines is jeopardized by H_2S impurities in the natural gas, which is prone to react with vapor to form a corrosive environment, thus producing stress corrosion in pipelines. According to Sosa et al. [2, 3], five pipeline rupture accidents caused by corrosion occur worldwide per year. Hence, the analysis of mechanical properties and fracture toughness of X80 pipelines in operational conditions is crucial for the reliability assessment of oil-and-gas equipment components and prediction of their service life.

There are numerous studies on the stress corrosion cracking (SCC) resistance of X80 pipeline steel due to its wide application. Thus, Xi et al. [4] investigated H_2S-induced SCC behavior of X80 pipeline steel and its welded joints using the three-point bending tests. Wang et al. [5] used the welded joints of X80 pipeline steel to prepare wedge-open loading (WOL) specimens and then conducted constant-displacement SCC tests in the H_2S environment. The threshold stress intensity factor (SIF) for SCC ($K_{\mathrm{I},SCC}$) and crack growth rates were determined for the base metal, weld seam, and heat-affected zone in the tests. Chen et al. [6] categorized SCC types and a principle of buried X80 oil pipelines, as well as examined the influence of material, stress and environmental factors (temperature, applied potential, and cathodic protection) on the SCC behavior of X80 pipeline steel, and offered the respective protection measures.

This study is devoted to the X80 pipeline steel employed in the above project, given the particular operational conditions. After being exposed to air and H_2S corrosion,

specimens from X80 pipeline steel were tersted to determine their tensile and fracture properties. The respective resistance curve "crack opening displacement–crack extension" ($\delta - \Delta a$) and the characteristic values $\delta_{0.2BL}$ were obtained. The influence of H_2S corrosion on the crack growth resistance curve, fracture toughness and plastic work loss of the X80 pipeline steel was determined, providing the data support for its engineering application.

1. **Experimental**.

1.1. ***Material***. The X80 pipeline steel used in this study was obtained from pipelines in the West-East Gas Pipeline Project, China. The chemical compositions (wt.%) of the tested steel are illustrated in Table 1. The measured elastic modulus E is 206 GPa, tensile strength R_m is 767 MPa, yield strength $R_{p0.2}$ is 661 MPa. elongation A is 19.1%, and reduction of area Z is 77.7%.

Table 1

Chemical Composition of the Tested Steel (wt.%)

C	Si	Mn	P	S	Cr	Ni	Ti	Nb	V	Mo
0.065	0.27	1.82	0.011	0.0006	0.03	0.03	0.016	0.061	0.059	0.21

1.2. ***Specimen Geometry***. Specimens for tensile tests (Fig. 1a) and three-point bending tests (Fig. 1b) were designed according to the national standards GB/T 228.1-2010 [7] and GB/T 21143-2007 [8], respectively. The geometry of a standard specimen for three-point bending tests was employed. Given the actual wall thickness of pipeline ($t = 19$ mm), the specimen thickness was determined as 15 mm, while its width was $W = 30$ mm and length was $S = 120$ mm.

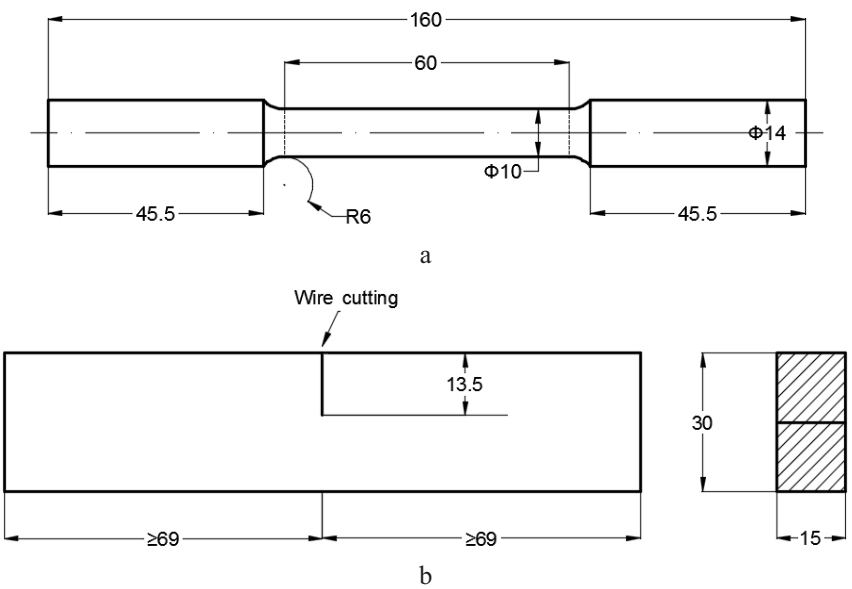

Fig. 1. Specimens for tensile (a) and three-point bending (b) tests.

In compliance with the above national standard [8], initial fatigue cracks of 2 mm-length were prefabricated using a high-frequency fatigue test machine, with the maximum load of 14.87 kN and the stress ratio $R = 0.1$.

1.3. ***Experimental Environment***. The X80 pipeline steel specimens were subjected to tensile tests and fracture toughness tests before and after H_2S corrosion at room temperature. Therein, the H_2S corrosion environment was the standard Class A H_2S corrosive solution, according to NACE International requirements [9–11], i.e., H_2S gas was injected into the aqueous solution containing 5% NaCl and 0.5% CH_3COOH until saturated (concentration $2300 \cdot 10^{-6}$ (volume fraction)), the rate of H_2S gas bubbling was 300 cm^3/min, per liter of test solution for the first 60 minutes. Thereafter, a positive pressure of H_2S in the test solution was measured by the iodometric titration. The corrosion process duration was 48 hours.

1.4. ***Experimental Steps***. Tensile tests were performed using a Zwick Z150 test machine, according to the national standard GB/T228.1-2010 [7]. The machine automatically recorded and plotted tensile force–displacement curves during the test. The elastic modulus, yield strength, tensile strength, elongation, reduction of area, and the total work of the stretching process were obtained after the test.

The multiple-specimen method was adopted for the test. Specifically, several specimens were loaded to varying displacement levels, which were preset. Then, they were unloaded, frozen in a liquid nitrogen, and broken. The original crack growth length a_0 and final crack growth Δa were measured, and the crack opening displacement δ was calculated. The blunting line equation of $\delta - \Delta a$ curves was $\delta = 1.87(R_m / R_{p0.2})\Delta a$ [8]; a line parallel to the blunting line was drawn at $\Delta a = 0.1$ mm, as the left boundary of the effective crack growth, and another parallel line was drawn at $\Delta a_{\max}$ as the right boundary. The effective crack growth area was quartered, each sub-area containing at least one data point. If there were data missing in a subarea, a data point would be added according to the test result of the adjacent sub-area. The test was terminated when six or more effective data points were obtained and they were evenly spaced. The loading process is shown in Fig. 2.

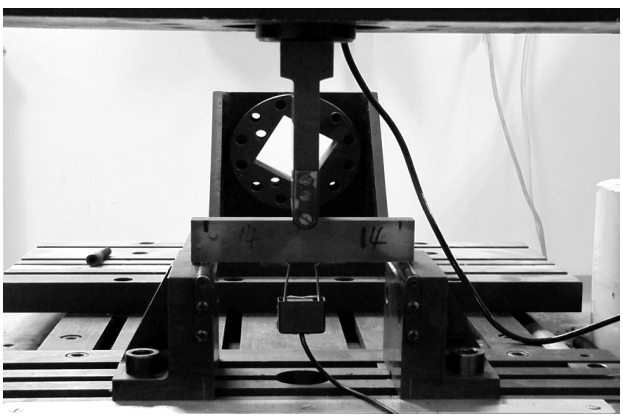

Fig. 2. Loaded specimen by using universal electronic testing machine.

For specimens subjected to the three-point bending test, δ is calculated as follows [8]:

$$\delta = \left[\left(\frac{S}{W}\right)\frac{F}{(BB_N W)^{0.5}} g_1\left(\frac{a_0}{W}\right)\right]^2 \left[\frac{(1-\nu^2)}{2R_{p0.2}E}\right] + \frac{[0.6\Delta a + 0.4(W - a_0)]V_P}{0.6(a_0 + \Delta a) + 0.4W + z}, \qquad (1)$$

where S and W are specimen length and width, respectively, F is the load at break point, B is the specimen thickness, B_N is the net specimen thickness between two side troughs ($B_N = B$ in this paper), g_1 is the SIF coefficient for three-point bending test specimens,

a_0 is the original crack length, ν is Poisson's ratio, $R_{p0.2}$ is the proof strength at 0.2% non-proportional extension of the material along the direction vertical to the crack plane at the test temperature, E is elastic modulus, Δa is the final crack growth increment, V_p is the plastic component of crack opening displacement (COD), and z is the thickness of an extensometer knife edge used for the COD measurement.

A line parallel to the blunting line is drawn at $\Delta a = 0.2$ mm, and its intersection with the resistance curve is defined as $\delta_{Q0.2BL}$. The validity of $\delta_{Q0.2BL}$ is controlled by the following conditions: (i) there is at least one data point between 0.1 and 0.3 mm offset lines parallel to the blunting line, and at least two data points between 0.1 and 0.5 mm offset lines; (ii) $\delta_{Q0.2BL} < \delta_{\max} = (W - a_0)/20$; (iii) the slope of resistance curve at its intersection with the 0.2 mm offset line satisfies the inequality $1.87\left(\frac{R_m}{R_{p0.2}}\right) > \left[2\left(\frac{d\delta}{da}\right)\right]_{0.2BL}$. If $\delta_{Q0.2BL}$ satisfies the above conditions, the obtained $\delta_{Q0.2BL}$ is insensitive to the scale effect.

2. **Experimental Results**.

2.1. ***Tensile Properties of X80 Pipeline Steel after H_2S Pre-Corrosion***. Tensile properties of X80 pipeline steel were tested after pre-corrosion. The engineering stress–strain curve was recorded, as seen in Fig. 3, while Table 2 lists the material tensile properties.

Table 2

Tensile Properties of X80 Pipeline Steel before and after H_2S Pre-Corrosion

Specimen No.	E, GPa	$R_{p0.2}$, MPa	R_m, MPa	A, %	Z, %	W_B, J
Before corrosion 1#	206.0	634.0	773	20.0	78.7	522.49
Before corrosion 2#	199.0	647.0	775	18.8	76.7	478.50
Average	202.5	640.5	774	19.4	77.7	500.50
Saturated H_2S, 48h, 1#	212.0	658.0	782	12.9	44.1	379.45
Saturated H_2S, 48h, 2#	209.0	659.0	782	13.7	41.0	402.61
Average	210.5	658.5	782	13.3	42.55	391.03

Note. Here and in Table 6: W_B is total work of the stretching process.

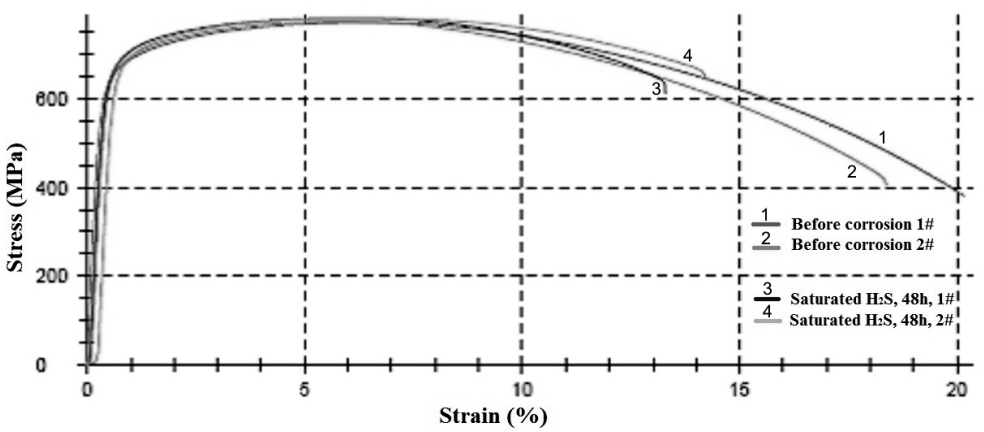

Fig. 3. Engineering stress–strain curve of X80 pipeline steel before and after H_2S pre-corrosion.

2.2. ***Crack Initiation Toughness $\delta_{0.2BL}$ at Stable Crack Growth and Its Validity Judgment***. The $\delta - \Delta a$ resistance curve and crack initiation toughness $\delta_{0.2BL}$ were obtained for the X80 pipeline steel specimens subjected to three-point bending test before and after H_2S corrosion. Tables 3 and 4 show the test results of each specimen before and after H_2S corrosion, respectively. Figure 4 shows the $\delta - \Delta a$ resistance curve. Figure 5 displays the fracture of specimens exposed in air and corroded by H_2S.

Table 3

Test Results for Specimens Exposed in Air

Sample number	B, mm	W, mm	S, mm	F, kN	g_1	ν	$R_{p0.2}$, MPa	E, GPa	a_0, mm	Δa, mm	V_p, mm	z, mm	δ, mm
A1	15.02	30.10	120	31.56	2.58	0.3	661	206	14.73	0.63	2.81	2.0	0.81
A2	15.03	30.00	120	28.50	2.62	0.3	661	206	14.84	1.34	3.78	2.0	1.05
A3	15.00	30.20	120	24.09	2.62	0.3	661	206	14.81	3.01	5.03	2.0	1.36
A4	14.99	30.20	120	26.81	2.66	0.3	661	206	15.01	2.15	4.63	2.0	1.25
A5	15.10	30.02	120	27.86	2.66	0.3	661	206	15.04	0.83	2.74	2.0	0.76
A6	15.01	30.02	120	27.07	2.58	0.3	661	206	14.71	2.28	4.18	2.0	1.15

Table 4

Test Results for the Specimens after H_2S Pre-Corrosion

Sample number	B, mm	W, mm	S, mm	F, kN	g_1	ν	$R_{p0.2}$, MPa	E, GPa	a_0, mm	Δa, mm	V_p, mm	z, mm	δ, mm
3#	15.10	29.82	120	27.88	2.58	0.3	661	206	14.57	0.25	0.78	2.0	0.26
4#	14.90	29.80	120	27.93	2.54	0.3	661	206	14.54	0.51	1.42	2.0	0.43
5#	15.02	29.72	120	29.40	2.54	0.3	661	206	14.43	0.35	1.13	2.0	0.36
8#	15.11	30.10	120	16.46	2.66	0.3	661	206	15.08	1.18	1.90	2.0	0.52
11#	15.00	30.00	120	19.87	3.63	0.3	661	206	15.90	1.87	2.31	2.0	0.61
12#	15.09	29.92	120	16.10	4.43	0.3	661	206	16.21	2.98	3.03	2.0	0.76

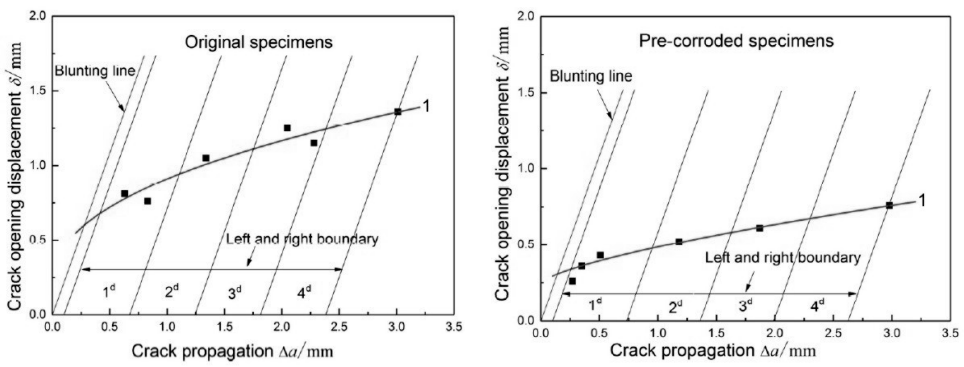

a b

Fig. 4. $\delta - \Delta a$ resistance curves (*1*) of original specimens (a) and saturated H_2S pre-corroded specimens (b).

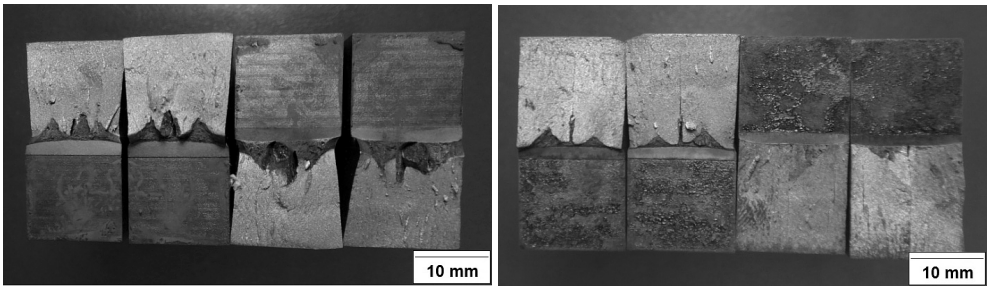

a b

Fig. 5. Fracture surfaces of original specimens (a) and saturated H_2S pre-corroded specimens (b).

In Fig. 4b, a parallel line passing through the passivation line at $\Delta a = 0.1$ mm is defined as the left boundary of the effective crack growth length, and the parallel line passing through $\Delta a_{\max}$ as the passivation line is defined as the right boundary of the effective crack growth length. The entire dataset falls between the left and right boundaries. At least six data points are required to define the *R*-curve, and when fitting the *R*-curve, there is at least one data point in the four equally spaced crack extension regions (1^d, 2^d, 3^d, and 4^d).

The resistance curve was fitted by the three-parameter exponential equation recommended by the national standard [8]. The resistance curve equation and crack initiation toughness after exposure to air and H_2S corrosion were finally obtained as follows:

Before H_2S corrosion: $\delta = 0.20041 + 0.7093\Delta a^{0.44416}$.

After H_2S corrosion: $\delta = 0.24544 + 0.23993\Delta a^{0.69532}$.

A line parallel to the blunting line was drawn at $\Delta a = 0.2$ mm. According to its intersection with the resistance curve, the $\delta_{Q0.2BL}$ after exposure to air and H_2S corrosion was obtained separately. Figure 6 and Table 5 summarize the data distribution and their validity judgment.

Table 5

Values of $\delta_{Q0.2BL}$ and Their Validity

Test condition	Data distribution requirements	$\delta_{Q0.2BL}$, mm	$\delta_{\max}$, mm	$1.87\left(\frac{R_m}{R_{p0.2}}\right)$	$\left[2\left(\frac{d\delta}{d(\Delta a)}\right)\right]_{0.2BL}$	Validity judgment
Original	Meet conditions	0.732	0.749	2.26	0.732	Valid
Pre-corroded	Meet conditions	0.364	0.686	2.22	0.364	Valid

Table 5 shows that $\delta_{Q0.2BL}$ values of the specimens exposed in air and corroded by H_2S are both valid. Thus, the crack initiation toughness of X80 pipeline steel for stable crack growth in these two test condition attains the following values:

Before H_2S corrosion: $\delta_{0.2BL} = 0.732$ mm; after H_2S corrosion: $\delta_{0.2BL} = 0.364$ mm.

3. **Discussion**.

3.1. ***Comparison of Tensile Properties***. The tensile test results of X80 pipeline steel before and after H_2S corrosion were averaged and compared (Table 6). It can be seen that the elastic modulus, yield strength, and tensile strength raised slightly after H_2S corrosion, but the overall variations were small (all within 4%). However, H_2S produced a significant

Table 6

Strength and Plasticity Indices of X80 Pipeline Steel before and after H_2S Corrosion

State of specimen	E, GPa	$R_{p0.2}$, MPa	R_m, MPa	A, %	Z, %	W_B, J
Before corrosion	202.5	640.5	774	19.4	77.70	500.50
Corroded by saturated H_2S for 48 h	210.5	658.5	782	13.3	42.55	391.03
Difference	+8.0	+18.0	+8.0	−6.1	−35.15	−109.47
Percentage difference	3.95%	2.81%	1.03%	31.44%	45.23%	21.87%

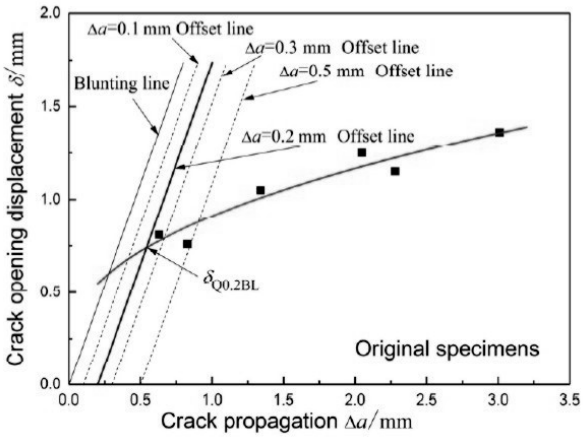

a

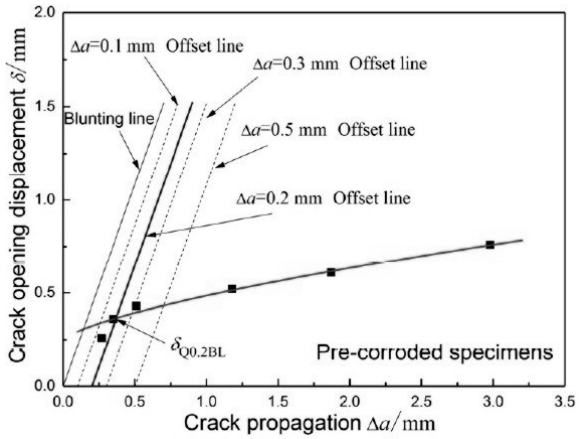

b

Fig. 6. The value of $\delta_{Q0.2BL}$ and validity judgment of original specimens (a) and saturated H_2S pre-corroded specimens (b).

influence on the plasticity characteristics. Specifically, the elongation, reduction of area, and total mechanical energy of the stretching process decreased by 31, 45, and 21%, respectively, after H_2S corrosion. This finding accords with other researchers' achievements [12]. The reason for these variations of plasticity characteristics is as follows. Hydrogen ions are

generated through electrolysis in the H_2S corrosive solution and then infiltrate into the metal material. Once meeting such hydrogen traps as inclusions, grain boundaries, and cavities, hydrogen atoms will bind to these strong traps, leading to an increase of local hydrogen concentration and a ductility loss to the metal material [13]. As a result, both elongation and the reduction of area decline, while the total work done in the stretching process also declines.

3.2. ***Comparison of*** $\delta_{0.2BL}$. $\delta_{0.2BL}$ refers to the crack opening displacement at the intersection of the 0.2 mm offset line of blunting line and the resistance curve. The value characterizes the material's resistance against crack initiation and growth [14]. Test results indicate that the $\delta_{0.2BL}$ value of X80 pipeline steel in air was 0.74 mm, and it decreased to 0.365 mm after the corrosion of saturated H_2S, which implies more than a twofold reduction. This shows that H_2S corrosion significantly degraded the fracture toughness of X80 pipeline steel.

Crack opening displacement δ has a close relationship with the stress field of crack tip, the intensity of which can be described by SIF K. The critical SIF $K_{\mathrm{I}c}$ is the minimum SIF, at with an unstable crack growth occurs. It is a crucial parameter for measuring the fracture toughness of materials. In engineering, the crack initiation toughness $\delta_{0.2BL}$ under stable crack growth can be used to estimate the value of $K_{\mathrm{I}c}$.

According to [15, 16], δ can be reduced to the following form:

$$\delta = \frac{J}{kR_{p0.2}}, \tag{2}$$

where J is the experimental equivalent of J-integral and k is the crack opening displacement (COD) reduction factor, with the value range of 1.1–2.0.

The relationship between J and K is as follows:

$$J_{\mathrm{I}c} = \frac{K_{\mathrm{I}c}^2}{E'}, \tag{3}$$

where $K_{\mathrm{I}c}$ is the fracture toughness and $E' = E/(1-\nu^2)$ for plane strain.

It can be deduced from Eqs. (2) and (3) that

$$K_{\mathrm{I}c} = \sqrt{\frac{\delta_{0.2BL} kR_{p0.2} E}{1-\nu^2}}. \tag{4}$$

Set $k = 1.1$, and substitute the mechanical parameters of X80 pipeline steel and values of $\delta_{0.2BL}$ measured after exposure to air and H_2S corrosion into Eq. (6). This yields $K_{\mathrm{I}c} = 349\ \mathrm{MPa}\cdot\mathrm{mm}$ for the specimen in air and $K_{corr} = 245\ \mathrm{MPa}\cdot\mathrm{mm}$ for the H_2S-corroded specimen.

It was found that the fracture toughness $K_{\mathrm{I}c}$ of the steel X80 is reduced by 30% due to H_2S-corrosion, which further suggests that H_2S corrosive medium will make the steel more prone to brittle fracture. The reason is summarized as follows. High-stress area is produced at the crack tip during the specimen loading. Due to the stress-induced hydrogen diffusion, the hydrogen atoms in the metal will converge to the crack tip and form discoid atomic-hydrogen atmospheres (Cottrell atmospheres). The shearing component τ_H of the internal pressure works together with the shearing component induced by the external stress field, to promote the dislocation multiplication and movement in part of the crack tip. It will further promote local plastic deformations and reduce the material's fracture toughness [17, 18].

Wang et al. [19] also concluded that H_2S corrosive medium would degrade the fracture toughness of metal material according to the result that the critical SIF K_{Ic} of high-pressure cylinder material 4130 was 1.94 times higher than that after exposure to H_2S environment. As for the difference in the reduction scal with the present work, one reason is that different experimental materials show varying sensitivity to H_2S corrosive medium. Another reason is that specimens in this study were only subjected to the unstressed H_2S corrosion, i.e., static hydrogen charging. In such a case, hydrogen atoms enter the metal only through diffusion. But at ambient temperature the diffusion coefficient of hydrogen atoms is very low, so there are less hydrogen atoms reaching the bulk of specimens. In study [19], specimens were immersed into the corrosive environment during their loading, i.e., were subjected to a dynamic hydrogen-charging process. Besides the diffusion-induced mechanism, hydrogen atoms can also be carried to the inner layers of specimens by dislocations. The crack growth of specimens was caused by the hydrogen-stress coupling. During the dynamic hydrogen charging, the plastic deformation of specimen will induce massive dislocation slips. At this moment, the hydrogen atoms produced by the electrolysis will form atomic-hydrogen atmospheres near the dislocations and will be carried into the specimen bulk by these dislocations. The hydrogen atoms reaching the specimen surface due to electrolytic hydrogen charging will hence pour into the inner layers. Thus, a large number of hydrogen atoms will be enriched in the specimen quickly, finally resulting in the hydrogen-induced brittle fracture to the specimen.

3.3. ***Comparison of Crack Growth Resistance Curves***. Fracture resistance curves of the specimen in air and corroded by H_2S were compared, as seen in Fig. 7.

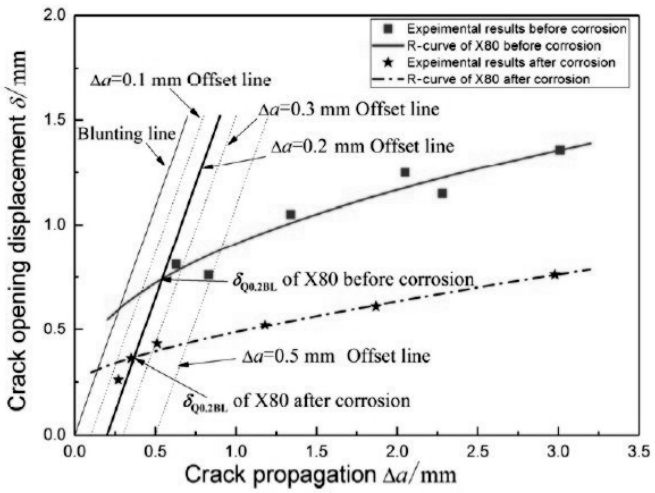

Fig. 7. Fracture resistance curves of X80 pipeline steel specimen before and after H_2S corrosion.

Crack growth resistance curve shows the material's resistance against crack initiation, and also reflects the variation of fracture toughness at crack tip with the crack length increment Δa. The crack growth resistance curves of X80 pipeline steel after exposure to air and H_2S corrosion were plotted. As shown in Fig. 7, the crack growth resistance of specimens after two treatments increased with the growth of crack, presenting a convex ascent curve. It means that X80 pipeline steel has a good toughness and can maintain a certain bearing capacity after crack initiation. The crack will grow to some extent from its initiation to the specimen's fracture. Araújo et al. [20] obtained the *R*-curves of API X52 pipeline steel, according to the ASTM E1820-01 standard [21]. In their test, along with the increase of crack length increment Δa, the COD also increased, but the increasing rate

declined gradually. The increasing trend of their resistance curve conforms to ours, further affirming findings of this study. It is seen in Fig. 7 that, regardless of the crack length, the resistance curve of the specimen in air is always located much higher than that of the H_2S-corroded specimen. It means that the X80 pipeline steel in air has a much better toughness than that subjected to H_2S corrosion. As the crack grows, the difference between the resistance curves of the specimens after varying treatments became greater. At the rear of the curve($\Delta a = 3$ mm), the difference of crack opening displacement was about 1.78 times. It suggests that the superior toughness of the material in air was enhanced by the growth of crack.

3.4. ***Comparison of Plastic Work of the Crack Growing Process***. For the plastic work required in the crack growing process (U_P), its value is equal to the area of the applied force–crack opening displacement curve. $F-V$ curves of two specimens (A3: exposed to air; 12#: corroded by H_2S) with similar crack growth ($\Delta a \approx 3$ mm) were compared, as shown in Fig. 8.

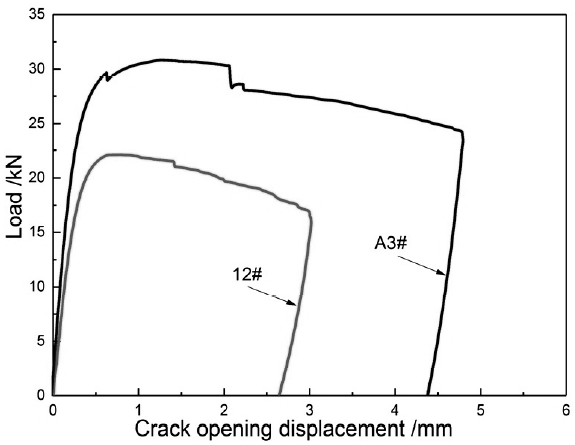

Fig. 8. Displacement–force curves of X80 pipeline steel specimens before and after H_2S corrosion.

As seen from the curves in Fig. 8, both the specimen in air and that corroded by H_2S presented a certain linear feature at the initial stage, during which the curve slope of the former was slightly higher. The difference between these two curves notably increased with the crack growth. Under condition of similar crack growth ($\Delta a \approx 3$ mm), the U_P value of H_2S-corroded specimen approached 52.5 kN·mm, and the U'_P value of uncorroded specimen approached 120 kN·mm, i.e., was 2.29 times higher that of the former one. This indicates that for the same crack growth, there was a large loss in the plastic work occurring in uncorroded specimens. It indirectly proves the superiority in fracture toughness of specimens in air over those corroded by H_2S. Chatzidouros et al. [22] studied the fracture toughness of X70 pipeline steel under conditions of electrolytic hydrogen charging, and plotted displacement– force curves for the specimens pretreated by air and corrosive media of different hydrogen concentration. They drew the similar conclusion as this study, that is, with an increase in hydrogen concentration, the plastic work required for the crack growth process decreased gradually. Thus, hydrogen corrosion would deteriorate the pipeline steel's fracture toughness.

A comparison was made between stretching and crack growth processes. It was found that, compared with uncorroded specimen, the total work carried out on the specimen in the stretching and crack growth processes declined by 22 and 56%, respectively, after corrosion. Obviously, the defective specimen had a greater energy loss than the specimen with a smooth surface. It is because hydrogen atoms are mostly concentrated at the

specimen surface after H_2S corrosion. After the test began, these surface hydrogen atoms entered into the specimen by the stress-induced diffusion and dislocation mechanisms. During the stretching, the internal stresses in the specimen were relatively uniform. The same was true for the hydrogen atoms redistributed inside the specimen by the stress-induced diffusion. However, for the pre-cracked specimens, there was a high-stress area at the crack tip after loading. Abundant hydrogen atoms converged in this area, thus increasing the ductility loss, as compared to the stretching process.

Conclusions

1. The ultimate tensile strength R_m and the proof strength $R_{p0.2}$ of X80 pipeline steel showed no large differences before and after H_2S corrosion for unnotched samples in standard tensile testing. However, such properties as fracture elongation and reduction of area were significantly lower for the corroded specimens.

2. The $\delta - \Delta a$ resistance curve and crack initiation toughness $\delta_{0.2BL}$ were experimentally obtained for the X80 pipeline steel pretreated in air and H_2S corrosive medium under conditions of stable crack growth. The following results were obtained: for the specimen in air, the resistance curve equation was $\delta = 0.20041 + 0.7093\Delta a^{0.44416}$, and the crack initiation toughness was $\delta_{0.2BL} = 0.732$ mm; for the H_2S-corroded specimen, the resistance curve equation was $\delta = 0.24544 + 0.23993\Delta a^{0.69532}$, and the crack initiation toughness was $\delta_{0.2BL} = 0.364$ mm.

3. The resistance curve of the specimen exposed in air was located much higher than that after H_2S corrosion. The crack initiation toughness, fracture toughness, and plastic work in the crack growing process of the specimen in air were 2.02, 1.42, and 2.29 times higher than those of H_2S-corroded specimens, respectively. Thus, H_2S corrosion significantly degraded the fracture toughness of X80 pipeline steel.

Acknowledgments. This article is supported by National Key Research and Development Program of China (Project No. 2016YFC0801905-16).

1. L. Zheng and S. Gao, "Research and trial production of X80 pipeline steel with high toughness using acicular ferrite," *Engineering*, **3**, No. 3, 91–94 (2005).
2. E. Sosa and J. Alvarez-Ramirez, "Time-correlations in the dynamics of hazardous material pipelines incidents," *J. Hazard. Mater.*, **165**, Nos. 1–3, 1204–1209 (2009).
3. J. L. Alamilla, M. A. Espinosa-Medina, and E. Sosa, "Modelling steel corrosion damage in soil environment," *Corros. Sci.*, **51**, No. 11, 2628–2638 (2009).
4. Y. T. Xi, D. X. Liu, H. P. Cai, et al., "Stress corrosion cracking behavior of domestic X80 pipeline steel in H_2S environment," *Corros. Sci. Prot. Technol.*, **19**, No. 2, 103–105 (2007).
5. B. Y. Wang, L. X. Huo, Y. F. Zhang, and D. P. Wang, "H_2S stress corrosion test of welded joint for X80 pipeline steel," *Pres. Ves. Technol.*, **23**, No. 7, 15–18 (2006).
6. Y. Chen, J. Y. Fei, B. H. Wan, and L. Wang, "Stress corrosion crack of buried X80 oil pipeline and its protection," *Hot Work. Technol.*, **40**, No. 22, 55–59 (2011).
7. *GB/T 228.1-2010. Metallic Materials – Tensile Testing – Part 1: Method of Test at Room Temperature* [in Chinese], Chinese National Standard (2010).
8. *GB/T 21143-2007. Metallic Materials – Unified Method of Test for Determination of Quasistatic Fracture Toughness* [in Chinese], Chinese National Standard (2007).
9. *NACE TM0177-2005. Laboratory Testing of Metals for Resistance to Sulfide Stress Cracking and Stress Corrosion Cracking in H_2S Environments*, NACE International (2005).

10. *NACE MR0175-2003. Standard Material Requirements – Metals for Sulfide Stress Cracking and Stress Corrosion Cracking Resistance in Sour Oilfield Environments*, NACE International (2003).
11. *NACE TM0284-2011. Evaluation of Pipeline and Pressure Vessel Steels for Resistance to Hydrogen-Induced Cracking*, NACE International (2011).
12. P. Y. Wang, J. Wang, S. Q. Zheng, et al., "Effect of H_2S/CO_2 partial pressure ratio on the tensile properties of X80 pipeline steel," *Int. J. Hydrogen Energ.*, **40**, No. 35, 11925–11930 (2015).
13. T. Depover, E. Van den Eeckhout, and K. Verbeken, "Hydrogen induced mechanical degradation in tungsten alloyed steels," *Mater. Charact.*, **136**, 84–93 (2018).
14. *GB/T 8650-2015. Evaluation of Pipeline and Pressure Vessel Steels for Resistance to Hydrogen-Induced Cracking* [in Chinese], Chinese National Standard (2016).
15. C. Chen, Q. G. Cai, and R. Z. Wang, *Engineering Fracture Mechanics* [in Chinese], National Defense Industry Press, Beijing (1977).
16. Q. F. Li, *Fracture Mechanics and the Engineering Application* [in Chinese], Harbin Engineering University Press, Harbin (2007).
17. W. Y. Chu, L. J. Qiao, J. X. Li, et al., *Hydrogen Embrittlement and Stress Corrosion Cracking* [in Chinese], Science Press, Beijing (2013).
18. Q. Hong and Y. X. Chen, "Effects of static and dynamic hydrogen charging on tensile properties of SM490B clean steel," *Shanghai Met.*, **34**, No. 1, 25–28, 37 (2012).
19. J. Wang, X. Y. Li, and Y. L. Zhang, "Low cycle fatigue crack growth rate in H_2S environments," *J. Mech. Strength*, **31**, No. 3, 972–978 (2009).
20. A. A. de Araújo, F. L. Bastian, and E. M. Castrodeza, "CTOD-R curves of the metal-clad interface of API X52 pipes cladded with an Inconel 625 alloy by welding overlay," *Fatigue Fract. Eng. M.*, **39**, No. 12, 1477–1487 (2016).
21. *ASTM E1820-01. Standard Test Method for Measurement of Fracture Toughness*, ASTM International, West Conshohocken, PA (2001).
22. E. V. Chatzidouros, V. J. Papazoglou, T. E. Tsiourva, and D. I. Pantelis, "Hydrogen effect on fracture toughness of pipeline steel welds, with in situ hydrogen charging," *Int. J. Hydrogen Energ.*, **36**, No. 19, 12626–12643 (2011).

Received 15. 03. 2018